



# Macroporous carbon coatings through carbonization of emulsion-templated poly(dicyclopentadiene) on metal substrates

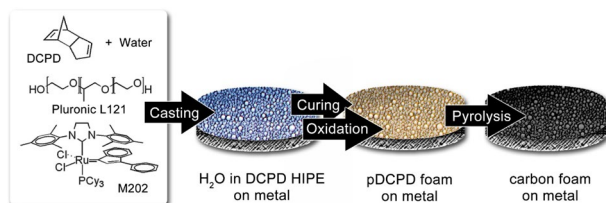
Sebastijan Kovačič<sup>1</sup> · Katharina Gruber<sup>2</sup> · Bernd Fuchsbichler<sup>2</sup> · Martin Schmuck<sup>2</sup> · Christian Slugovc<sup>3</sup>

Received: 19 December 2022 / Accepted: 15 February 2023 / Published online: 23 March 2023  
© The Author(s) 2023

## Abstract

In this article, we demonstrate the fabrication of thin and macroporous carbon coatings that adhere to various metal substrates such as nickel- or aluminum-based foils or meshes. The coating process is a combination of emulsion-templating and the doctor-blade method, which allows to prepare up to 350  $\mu\text{m}$  thick poly(dicyclopentadiene) membranes with a polyHIPE (polymerized high internal phase emulsions) architecture. Carbonization of these poly(dicyclopentadiene) membranes directly on the metal substrates resulted in up to 30- $\mu\text{m}$ -thick foamy carbon coatings that retain the highly porous architecture and flexibility. Subsequently, carbon foam-coated Ni-foils were filled with elemental sulfur by a melt diffusion technique. A macroporous carbon coating supported sulfur loadings up to 65 wt%, obtaining cathodes for galvanostatic cycling experiments in Li–S cells. The latter revealed discharge capacities higher than 800  $\text{mA h}^{-1}$  according to the sulfur mass. With our approach, the final assembly of the electrodes is greatly simplified because no binders or conductive fillers are required.

## Graphical abstract



**Keywords** Emulsion-templating · Carbonization · Ring-opening metathesis polymerization · Electrodes · Li–S batteries

## Introduction

The thermoset poly(dicyclopentadiene) (pDCPD), produced by ring-opening metathesis polymerization (ROMP), is characterized by excellent mechanical properties, i.e., high toughness and stiffness, offers high temperature and corrosion resistance, and excellent stability to chemicals [1]. Current research interest in pDCPD-based materials includes their preparation by additive manufacturing techniques [2–4], materials for the microelectronic industry [5] and introducing degradability into the material [6]. Porous pDCPD networks are also known and can be prepared either by polymerization induced phase separation, supercritical drying of wet polymer gels, block copolymer-, or emulsion-templating, to name a few [1]. The emulsion-templating

✉ Sebastijan Kovačič  
sebastijan.kovacic@ki.si

✉ Christian Slugovc  
slugovc@tugraz.at

<sup>1</sup> Department of Inorganic Chemistry and Technology, National Institute of Chemistry, Hajdrihova 19, 1000 Ljubljana, Slovenia

<sup>2</sup> VARTA Innovation GmbH, Stremayrgasse 9, 8010 Graz, Austria

<sup>3</sup> Institute for Chemistry and Technology of Materials, Technische Universität Graz, Stremayrgasse 9, 8010 Graz, Austria

approach is, in the context of this work, of particular interest. In this case, high internal phase emulsions (HIPEs) are used as structural templates and porous polymer monoliths known as “polyHIPEs” are generated [7, 8]. PolyHIPEs are typically single-piece polymer monoliths characterized by a unique 3D-interconnected microcellular porous morphology, tunable mechanical properties, and diverse chemistry. The main advantage of polyHIPEs, is the tunability of their porous properties, i.e., pore volume, size, and interconnectivity, simply by affecting the emulsion system with changes in either the phase volume ratio, surfactant, or polymerization system. The materials are attractive for a wide range of applications including e.g., filter membranes, adsorbents, supports for solid phase chemistry, scaffolds for tissue engineering, and supports for CO<sub>2</sub> capture [9]. PolyHIPEs prepared by ROMP exhibit particularly favorable mechanical properties [10] and were used as separators in Li-ion batteries [11], as oxygen scavenger materials [12], and in mixed matrix membranes as host for metal organic frameworks [13, 14].

PolyHIPEs have also served as precursors for the generation of monolithic macroporous carbons through carbonization [15, 16]. PolyHIPE-templated carbons have been prepared from poly(styrene) and poly(divinylbenzene) [17], poly(acrylonitrile) [18], furfural-phloroglucinol [19], tannin [20], Kraft black liquor [21, 22], 2,5-dihydroxy-1,4-benzoquinone and urea [23], or resorcinol–formaldehyde resins [24]. Above that, the preparation of porous carbon composites [25–27] or hierarchically porous carbons [23–28] through carbonization of polyHIPEs templates has been developed. PolyHIPE-templated carbon have been used in various applications such as catalysis [29–31], CO<sub>2</sub> capture [27, 32], or as carbon component in battery electrodes [33–35]. Using them in lithium-sulfur (Li–S) batteries revealed a minimized lithium polysulfide dissolution during cell operation [36, 37]. However, hitherto described Li–S cells using such porous carbons suffer from modest sulfur utilization and/or limited interface contact with the metallic current collectors [38, 39]. To circumvent the latter problem in particular, there is considerable interest in developing free-standing polyHIPE-templated carbon electrodes. In such an electrode, the monolithic carbon framework serves either as an active material or as a 3D current collector [40]. Another important aspect is that the free-standing polyHIPE-templated electrodes can be developed without binder.

The use of carbon coatings on various current collectors have been reported to significantly improves the performance of the electrodes, as such an arrangement significantly reduces the contact resistance at the current collector-carbon interface [41, 42]. Various coating processes are used to produce carbon-coated current collectors. On a laboratory scale, coating is usually done by the doctor blade method, in which slurries containing carbon powder, carbon black, or fine

graphite as a conductive additive, together with active material and a binder, are casted onto the current collector surface to form homogeneous films [43]. Although carbon-coated current collectors have better rate performance, more stable cycling, and lower area-specific resistance the use of binders and solvents for their preparation is still required. Therefore, in this article, an emulsion-templating is used in combination with a doctor-blade method, and highly porous 150 to 300 μm thick pDCPD membranes are prepared directly on various metal substrates such as nickel- or aluminum-based foils and meshes. Carbonization at 600 °C resulted in well-defined carbon coatings with a foamy structure and a thickness of ~30 μm adhering to metallic current collectors. As a use case, the developed carbon-coated current collectors are filled with elemental sulfur and cathodes for Li–S cells are assembled and tested.

## Results and discussion

Based on prior work, we herein selected a HIPE formulation consisting of dicyclopentadiene (DCPD, 20 vol%) as the external phase, water (80 vol%) as the internal phase, Pluronic®L121 as the surfactant (7 vol% with respect to DCPD), and M202 as the ring-opening metathesis polymerization initiator (Fig. 1). pDCPD foams synthesized from this HIPE composition have proven to be an advantageous compromise between maximum porosity, small structural sizes (void and window sizes), and good mechanical stability [44–46]. Furthermore, the carbonization of pDCPD foams derived from this particular formulation has been previously described in detail and the resulting carbon foams have been thoroughly characterized [47].

However, in order to obtain DCPD-based carbon foam in any shape, prior oxidative treatment (additional crosslinking) is of utmost importance to remove the thermoplastic properties and thus increase the glass transition

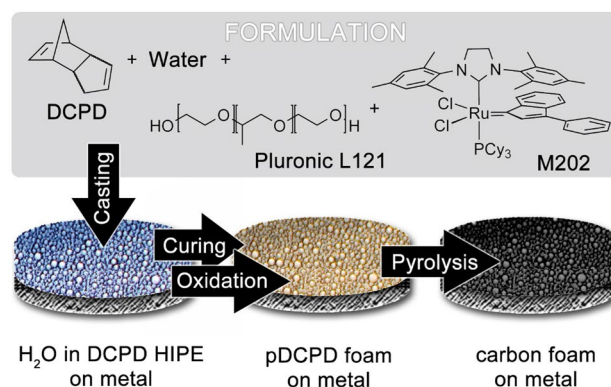


**Fig. 1** Formulation and most important steps in the preparation of the carbon foam coated metals

temperature of pDCPD. Otherwise, the pDCPD network melts at higher temperatures and the foam loses its porous structure [47]. Normally, the oxidation is simply carried out in air at room temperature without using organic solvents, toxic reagents or catalysts. During this time, the pDCPD network is oxidized, producing various oxidation products, e.g., hydroperoxides, carbonyls, etc. [48], which cause additional crosslinking. To demonstrate the versatility of the synthetic approach, we have continued our studies into the preparation of stable carbon coatings with a foamy structure that adhere to various metal substrates. We first attempted the coating of nickel substrates. HIPEs stabilized with 7 vol. % of the surfactant were carefully spread on the Ni-foil substrate by the doctor-blade method in thicknesses of 150, 250 and 350  $\mu\text{m}$  and then covered with a glass plate to ensure direct contact with the HIPE [46]. The as-prepared samples were then polymerized in an oven at 80  $^{\circ}\text{C}$  for 2 h. Prior to oxidation, polyHIPE-coated Ni-foils were cut to obtain coin cell electrodes of suitable size (Fig. 2A), which were later used for electrochemical measurements. After the usual oxidation process described above, the oxidized polyHIPE-coated Ni-foils were carbonized at 600  $^{\circ}\text{C}$  to obtain a carbon coating on the Ni-foil (Fig. 2C and E). Carbon coatings obtained from polyHIPE-coated films with thicknesses of 250 and

350  $\mu\text{m}$  peeled off from the metal substrate, so only polyHIPE films with a thickness of 150  $\mu\text{m}$  were used for further studies.

Another problem was also a higher carbonization temperature, which causes the carbon coating to detach from the substrate regardless of thickness. As expected, carbonization results in a throughout open-pore carbon coating that adhered to the Ni-foil with a thickness of up to 30  $\mu\text{m}$  (Fig. 2D–F). A combination of the pronounced shrinkage of the polyHIPE during carbonization above 600  $^{\circ}\text{C}$  and the thermal expansion of the Ni-foil ( $13.4 \times 10^{-6} \text{ K}^{-1}$  at 20  $^{\circ}\text{C}$  and  $16.8 \times 10^{-6} \text{ K}^{-1}$  at 523  $^{\circ}\text{C}$ ) is likely responsible for the carbon coatings peeling off. To circumvent the exfoliation problems during carbonization and to obtain thicker carbon coatings, a Ni-mesh was used as substrate and HIPEs were cast by the doctor blade method, initially with thicknesses of 150  $\mu\text{m}$ . In this case, HIPE fills the interspaces between the wires and after ROMP the whole Ni-mesh is embedded in the polyHIPE. To achieve good adhesion, HIPE must be spread over the mesh within the first five minutes after adding the initiator to HIPE. After curing, the adhesion and open surface morphology of the polyHIPE were found well preserved (Fig. 3A and B). However, shrinkage during carbonization caused the carbon coating to partially peel off from the Ni-mesh. From SEM imaging, it appeared

**Fig. 2** Photo of oxidized polyHIPE coating (A) and carbon coated Ni-foil (B); SEM images of Ni-foil (C–E): side view of the carbon coating stacked to the Ni-foil (C); interior morphology of the carbon coating (D); plan view of the carbon coating stacked to the Ni-foil (E)

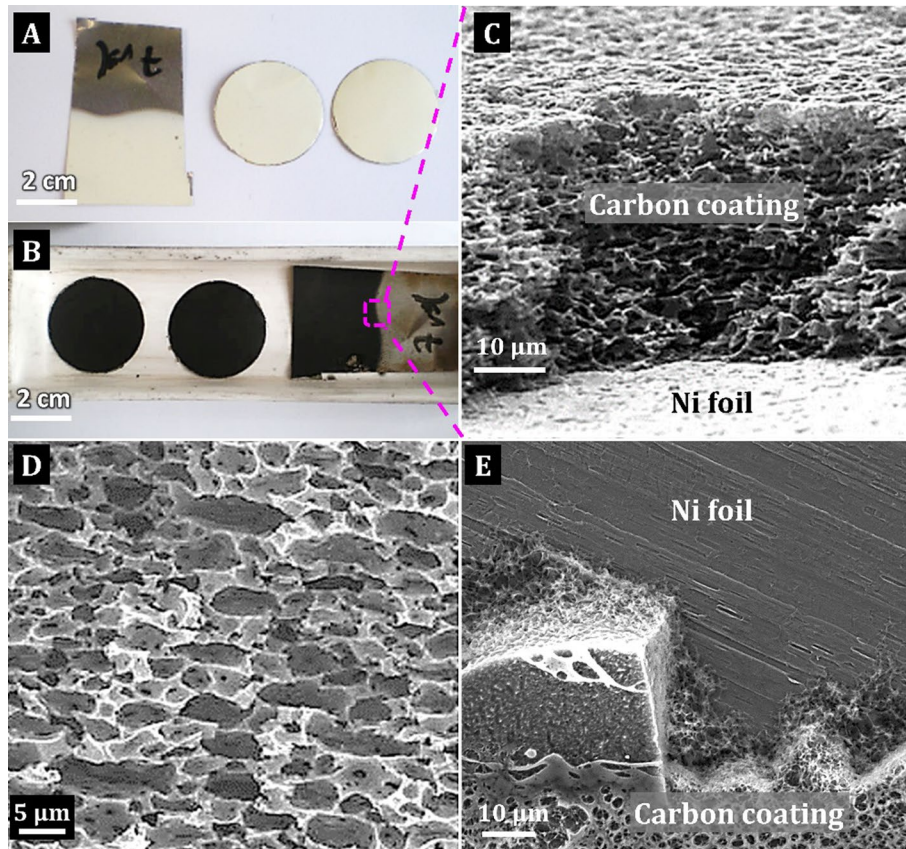
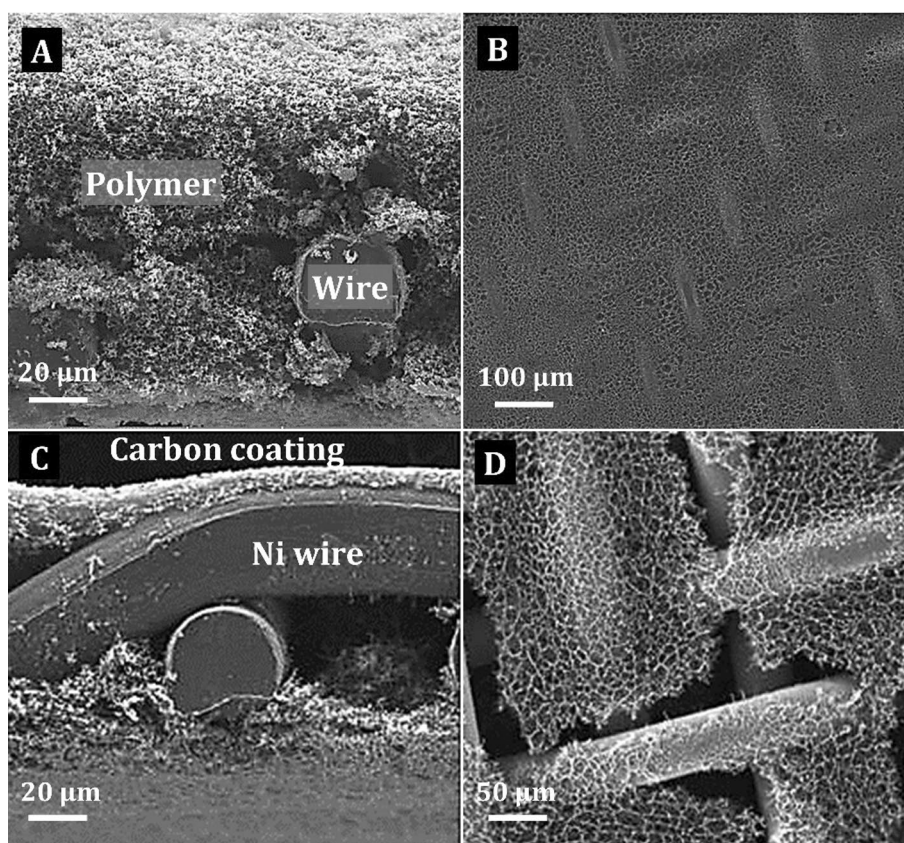


**Fig. 3** SEM images of Ni-mesh (A–D): side view of the polyHIPE polymer interpenetrated within the Ni mesh (A); surface morphology of the polyHIPE polymer within the Ni mesh (B); side view of the carbon-coated Ni mesh (C) surface morphology of the carbon-coated Ni mesh (D)



that in the areas where the Ni-mesh was fully coated with polyHIPE (both on the top surface and between the wires within the mesh), good adhesion of the carbon coating was achieved after carbonization. The opposite was found when the HIPE did not penetrate the mesh. In this case, the adhesion of the carbon coating was very poor and the layers pilled off (Fig. 3A and D). Presumably, an increased viscosity of HIPE, due to the polymerization already in progress, is thought to be responsible for this effect.

Next, carbon-coated Ni-foils were filled with elemental sulfur by a melt diffusion technique at 155 °C to obtain cathodes for galvanostatic cycling experiments. Considering an 80% porosity of the carbon coating and an average thickness of ~25 μm, a maximum filling would correspond to a sulfur loading of 3.6 mg cm<sup>-2</sup>. The actual sulfur loadings determined were 0.44 mg cm<sup>-2</sup> and 0.74 mg cm<sup>-2</sup>, corresponding to carbon/sulfur ratios of 46 and 60 by weight, respectively, indicating a certain number of macropores within the carbon coat not filled. However, despite the incomplete sulfur filling galvanostatic cycling of the cathodes was performed in pouch cells, using 0.014 cm<sup>3</sup> of electrolyte per mg of sulfur (0.014 cm<sup>3</sup>/mg S) and cycled between 1.8 to 2.4 V (vs Li/Li<sup>+</sup>) at a rate of 0.1 C, as shown in Fig. 3A. Please note that all capacity values are given in terms of mAh g<sup>-1</sup> per sulfur mass. Initial discharge capacities were in the range of over 800 mAh g<sup>-1</sup> in the first cycles, regardless of sulfur

loading, which was surprising and suggests that a comparable amount of sulfur was electrochemically accessible in both cases (Fig. 4A). An increase in specific capacitance to ~1000 mAh g<sup>-1</sup> was then observed in the first four cycles, most likely due to the repeated dissolution and precipitation processes during charging and discharging (Fig. 4A and B). During the next 40 cycles, the capacity then decreased somewhat and remained constant at about 550 mAh g<sup>-1</sup> until the 100th cycle (Fig. 4A).

The reason for this long-term stable capacity most likely lies in the unique, 3D-interconnected polyHIPE morphology of the HIPE-derived carbon coatings (Fig. 2C). Small throats (windows) connecting larger macropores (voids) apparently represent physical barriers that slow the dissolution of long-chain polysulfides (e.g., Li<sub>2</sub>S<sub>8</sub>, Li<sub>2</sub>S<sub>6</sub>) into the electrolyte during the redox process, which is also a known effect in porous carbon aerogels [49]. Another hypothesis is that empty macropores, which were initially not filled with sulfur, subsequently serve as empty areas into which long-chain polysulfides can diffuse before escaping into the electrolyte, slowing dissolution and prolonging their participation in the redox process, thus stabilizing the capacity. The latter is confirmed by the excellent retention of the initial charge–discharge capacity of the cathodes thus obtained, which have a high Coulombic efficiency (CE) of >96% and are reversible even

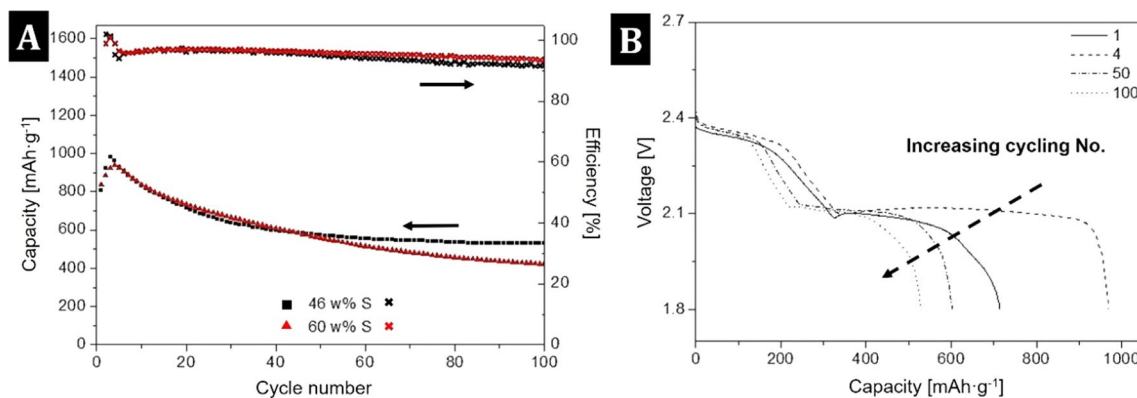


**Fig. 4** Cycle performance of carbon coated Ni-foil derived carbon/sulfur cathode with 46 wt. % and 60 wt. % sulfur (**A**); and corresponding specific voltage profile of 1st, 4th, 50th, 100th cycles of cathode materials with 46 wt. % sulfur (**B**)

after 100 cycles (Fig. 4A). This CE value is comparable to that of mesoporous carbon foam [50, 51], or carbon nano-tube-based composite cathodes with comparable sulfur loading [52]. Apparently, HIPE-derived carbon coatings have a favorable combination of porosity, pore size, 3D-interconnected structure, and good adhesion to the Ni-foil, which together ensure cathode performance despite a low specific surface area determined by the B.E.T. method ( $S_{\text{BET}}$  of  $3 \text{ m}^2 \text{ g}^{-1}$  determined for representative free standing carbon foam samples) and low sulfur loading (up to  $0.74 \text{ mg cm}^{-2}$ ) compared to other carbon materials in Li-S batteries with  $S_{\text{BET}}$  of more than hundreds of  $\text{m}^2 \text{ g}^{-1}$  [36–38, 53, 54]. Although the capacities achieved here are not particularly impressive in comparison to the state of the art [55], the results clearly demonstrate the feasibility of producing a binder and particulate carbon additive free electrode-architecture with this approach.

Finally, we also tested aluminum (Al) foils as metal substrates and design the cathode. Using Al instead of Ni would have the advantage of lower weight and a lower price of the final electrode. As described above, the HIPE was spread across the foils in thickness of  $150 \mu\text{m}$ , covered with a glass plate, polymerized in an oven at  $80 \text{ }^\circ\text{C}$  for 2 h. It was found that during polymerization of the HIPE and subsequent oxidation of the polyHIPE, the aluminum surface directly under or adjacent to the coating turned yellow compared to the bare Al-foil, indicating a possible reaction of the Al surface with the reactants from the HIPEs. EDX analysis confirmed that the oxygen content in these yellow areas at the aluminum surface increased threefold, from 9 to 27 wt%. PolyHIPE-coated foils were further carbonized, forming carbon coatings on the surface of the Al-foil, which was subsequently filled with elemental sulfur by melt diffusion (sulfur loading of  $0.70 \text{ mg/cm}^2$  was achieved). The cathodes thus prepared were then used for galvanostatic cycling experiments. Al-based cathodes showed no electrochemical activity, probably due to the formation of an electrically non-conductive

(oxide) layer on the surface, so the Al-substrate as current collector was not investigated further.

## Conclusion

In summary, emulsion templating combined by doctor blade method was used to fabricate highly porous, 150 to  $300 \mu\text{m}$  thick poly(dicyclopentadiene)membranes with a polyHIPE architecture adhered to various metal substrates such as nickel- or aluminum-based foils or meshes. Carbonization of these substrates coated with polyHIPEs at  $600 \text{ }^\circ\text{C}$  resulted in 10 s of micron thick carbon coatings on the metal surfaces with preserved polyHIPE structure. The developed carbon-coated Ni-foils were then filled with elemental sulfur (loadings of up to  $0.74 \text{ mg/cm}^2$ ) and cathodes for Li-S cells were designed and tested. Initial discharge capacities of over  $800 \text{ mAh g}^{-1}$  and capacity retention at about  $550 \text{ mAh g}^{-1}$  after 100 cycles at a rate of 0.1 C indicate that the cathodes are functional. Thus, our fabrication method, which enables binder-free, highly porous and flexible carbon coating directly on metallic current collectors, offers a promising opportunity for the development of electrodes for batteries.

## Experimental

Dicyclopentadiene (DCPD, Aldrich), Pluronic L-121 (poly(ethylene glycol)-block-poly(propylene glycol)-block-poly(ethylene glycol), Aldrich), the initiator ( $\text{H}_2\text{IMes}$ ) ( $\text{PCy}_3$ ) $\text{Cl}_2\text{Ru}$ (3-phenyl-indenylid-1-ene) (**M202**, Umicore,  $\text{H}_2\text{IMes} = N,N$ -bis(mesityl)-4,5-dihydroimidazol-2-yl),  $\text{PCy}_3 = \text{tricyclohexylphosphine}$ ), and toluene (p.a. Aldrich) were used as received.

**Synthetic procedure** Preparation of carbon coatings on metal substrates. The appropriate amounts of the

monomer DCPD (8.02 g), Pluronic L121 (0.62 g), and toluene ( $0.050 \text{ cm}^3$ ) were added to a 3-neck round bottom flask equipped with a mechanical stirrer and dropping funnel. The mixture was stirred at 400 rpm for 5 min and deionized water ( $33 \text{ cm}^3$ ) was added dropwise with continuous stirring. Initiator **M202** (8.1 mg) dissolved in toluene ( $0.25 \text{ cm}^3$ ) was then added, and the emulsion was stirred for an additional 1 min. DCPD-based HIPEs were then cast onto metal substrates (foils or meshes) using doctor blades with dimensioned slits between 150 and  $350 \mu\text{m}$ . The cast HIPEs were then covered with a glass lid to both ensure direct contact and prevent evaporation of DCPD (Fig. 5). As shown in Fig. 5 (black line), the spacer between the substrate and the glass plate was used to maintain the cast thickness of HIPE.

The samples were placed in an oven at  $80 \text{ }^\circ\text{C}$  for 2 h for polymerization. After 2 h, polymerization was complete and the lid was carefully removed. The polyHIPE adhering to the metal substrate was then oxidized in an oven at  $40 \text{ }^\circ\text{C}$  for 5 d. Subsequent carbonization at  $600 \text{ }^\circ\text{C}$  (heating ramp of  $4 \text{ K/min}$ ) of the now oxidized polyHIPE coating adhering to the metal substrate resulted in a macroporous carbon coating on the metal substrates.

**Sulfur infiltration** The sulfur content was 60 and 46% by weight, respectively, and was calculated based on the mass of the carbon layer obtained on the metal substrates. Sulfur was first dissolved in toluene and spread on carbonized samples in order to achieve a more homogeneous distribution. These were placed in a Büchi oven (Büchi glass oven B 585) and heated to  $155 \text{ }^\circ\text{C}$  under  $\text{N}_2$  gas. All together the sulfur infiltration process was accomplished within 30 min. As soon as sulfur melted (at  $120 \text{ }^\circ\text{C}$ ), it was completely soaked into the porous carbon material. The amount of sulfur inside the electrode was determined gravimetrically.

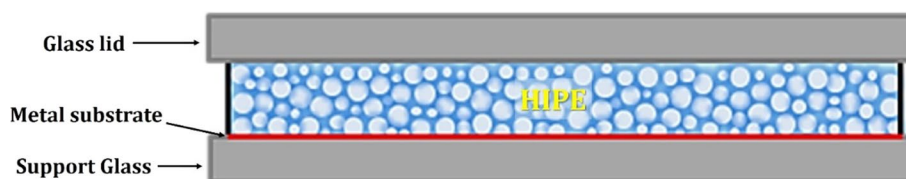
**Test cells for electrochemical measurements** Electrochemical measurements were performed in pouch cells. An acrylate/Al/PP compound foil served as casing of the pouch cells, with PP (polypropylene) layer being the inner layer. For standard Li–S cell measurements the electrode stack consisted of a  $2 \times 3 \text{ cm}^2$  sulfur/carbon working electrode and a metallic lithium stripe ( $100 \mu\text{m}$  or  $230 \mu\text{m}$ ) counter electrode, which were separated by a Celgard 2400 separator. The compound foil and the PP separator were dried under vacuum at  $90 \text{ }^\circ\text{C}$  prior to cell assembly. The current

collector tap of the sulfur/carbon electrode was cut out of the Al foil on which the active material layer was casted while a Ni-foil stripe, pressed on Lithium served as current collector tap at the negative electrode. Additionally, a reference electrode was placed between the current collector taps. The reference electrode consisted of a small piece of lithium foil wrapped around the Ni foil current collector tap and was in contact with the separator. After electrolyte addition, the compound foil was heat-sealed and a stripe of hot melt adhesive was additionally placed around the metal taps, ensuring the tightness of the sealing at metal/PP contact areas. Cell assembly was accomplished under inert atmosphere. If not stated differently, assembled cells were opened at ambient conditions and were instantaneously vacuum-sealed to eliminate argon from inside the cell. During electrochemical measurement, cells were placed in a jig to apply a moderate pressure on the electrode stack. A solution of 1 M lithium bis(trifluoromethanesulfonyl)imide (LiTFSI) –  $0.25 \text{ M LiNO}_3$  in a dimethoxyethane/dioxolane (1:1 w/w) mixture served as the liquid electrolyte. LiTFSI was dried at  $90 \text{ }^\circ\text{C}$  under vacuum for minimum of two days.  $\text{LiNO}_3$  was used as received. The obtained electrolytes showed a water content below 20 ppm. For electrochemical tests, the electrolyte amount in standard cells was held constant at  $0.014 \text{ cm}^3/\text{mg}$  of sulfur present at the applied electrode.

**Electrochemical characterization** Galvanostatic cycling and cyclic voltammetry measurements were performed using MACCOR Series 4000 battery tester and Biologic MPG -2, respectively. Unless otherwise specified, cut-off voltages for galvanostatic cycling measurements were set at 1.8 V and 2.6 V vs  $\text{Li}^+/\text{Li}$ , and the C rate was set at 0.1 C for a maximum of 200 cycles. The C-rate indirectly defines the charge and discharge current of the cell during galvanostatic measurement. Applying a C-rate of 1 corresponds to charging or discharging the cell within 1 h. Here the C-rate [ $\text{h}^{-1}$ ] was calculated based on the theoretical capacity of sulfur ( $1672 \text{ mAh g}^{-1}$ ) irrespective of the practical sulfur utilization. Measurements were controlled in full cell operation (control of cut-off voltages between working and counter electrode EWE–ECE).

**Characterization** Morphology investigations were performed using scanning electron microscopy. Scanning electron microscopy (Vega-3, Tescan) with a secondary electron detector was used to study the surface morphologies.

**Fig. 5** Schematic drawing of the process for the pDCPD coating of the metal substrates



The samples were coated with a ~3 nm thin gold layer to increase the electrical conductivity (Cressington 108 auto sputter coater). A tungsten cathode was used as the electron source and an accelerating voltage of 20 kV was applied. 3D images were generated using 3D software (Mex 5.1) by capturing SEM images with a tilt of 3°. In addition, an energy dispersive X-ray (EDX) detector was used to study the elemental composition.

**Acknowledgements** Support by Graz University of Technology (LP-03—Porous Materials@Work for Sustainability) and from VARTA Micro Innovation GmbH is kindly acknowledged. SK acknowledges the financial support from the Slovenian Research Agency (grant P2-0150). We thank Umicore for providing initiators.

**Funding** Open access funding provided by Graz University of Technology.

**Data availability** The data that support the findings of this study are available from the corresponding author, SK and CS, upon reasonable request.

## Declarations

**Conflicts of interest** The authors declare the following competing financial interest(s): some of the authors are also authors of a patent (WO 2013178371 A1) on using pDPCPD foams for the preparation of carbon foams.

**Open Access** This article is licensed under a Creative Commons Attribution 4.0 International License, which permits use, sharing, adaptation, distribution and reproduction in any medium or format, as long as you give appropriate credit to the original author(s) and the source, provide a link to the Creative Commons licence, and indicate if changes were made. The images or other third party material in this article are included in the article's Creative Commons licence, unless indicated otherwise in a credit line to the material. If material is not included in the article's Creative Commons licence and your intended use is not permitted by statutory regulation or exceeds the permitted use, you will need to obtain permission directly from the copyright holder. To view a copy of this licence, visit <http://creativecommons.org/licenses/by/4.0/>.

## References

- Kovačič S, Slugovc C (2020) *Mater Chem Front* 4:2235
- Leguizamón SC, Lyons K, Monk NT, Hochrein MT, Jones BH, Foster JC (2022) *ACS Appl Mater Interfaces* 14:51301
- Park J, Kwak SY (2022) *Commun Chem* 5:119
- Leguizamón SC, Cook AW, Appelhans LN (2021) *Chem Mater* 33:9677
- Wang J, Zhou DL, Lin X, Li JH, Han D, Bai H, Fu Q (2022) *Chem Eng J* 439:135737
- Husted KEL, Shieh P, Lundberg DJ, Kristufek SL, Johnson JA (2021) *ACS Macro Lett* 10:805
- Cameron NR, Sherrington DC (1996) *Adv Polym Sci* 126:163
- Zhang H, Cooper AI (2005) *Soft Matter* 1:107
- Zhang T, Sanguramath RA, Israel S, Silverstein MS (2019) *Macromolecules* 52:5445
- Kovačič S, Žagar E, Slugovc C (2019) *Polymer* 169:58
- Kovačič S, Kren H, Krajnc P, Koller S, Slugovc C (2013) *Macromol Rapid Commun* 34:581
- Vakalopoulou E, Borisov SM, Slugovc C (2020) *Macromol Rapid Commun* 41:1900581
- Kovačič S, Mazaj M, Jeselnik M, Pahovnik D, Žagar E, Slugovc C, ZabukovecLogar N (2015) *Macromol Rapid Commun* 36:1605
- Mazaj M, ZabukovecLogar N, Žagar E, Kovačič S (2017) *J Mater Chem A* 5:1967
- Edwards CJC, Hitchen DA, Sharples M (1988) Porous carbon structures and methods for their preparation. US Patent 4775655, Oct 4, 1988; (1987) *Chem Abstr* 107:120056
- Thongprachan N, Yamamoto T, Chaichanawong J, Ohmori T, Endo A (2011) *Adsorption* 17:205
- Wang D, Smith NL, Budd PM (2005) *Polym Int* 54:297
- Cohen N, Silverstein MS (2011) *Polymer* 52:282
- Brun N, Edembe L, Gounel S, Mano N, Titrici MM (2013) *Chemoschem* 6:701
- Szczurek A, Fierro V, Pizzi A, Celzard A (2014) *Carbon* 74:352
- Foulet A, Birot M, Backov R, Sonnemann G, Deleuze H (2016) *Mater Today Commun* 7:108
- Jalalian M, Jiang Q, Birot M, Deleuze H, Woodward RT, Bismarck A (2018) *React Funct Polym* 132:145
- Kapilov-Buchman K, Portal L, Zhang Y, Fechler N, Antonietti M, Silverstein MS (2017) *J Mater Chem A* 5:16378
- Gross AF, Nowak AP (2010) *Langmuir* 26:11378
- Woodward RT, Fam DWH, Anthony DB, Hong J, McDonald TO, Petit C, Shaffer MSP, Bismarck A (2016) *Carbon* 101:253
- Woodward RT, Markoulidis F, De Luca F, Anthony DB, Malko D, McDonald TO, Shaffer MSP, Bismarck A (2018) *J Mater Chem A* 6:1840
- Mazaj M, Bjelica M, Žagar E, ZabukovecLogar N, Kovačič S (2020) *Chemoschem* 13:2089
- Israel S, Levin M, Oliel S, Mayer D, Lerner I, Silverstein MS (2022) *Macromolecules* 55:1992
- Yi F, Gao Y, Li H, Yi L, Chen D, Lu S (2016) *Electrochim Acta* 211:768
- Zeng M, Wang Y, Liu Q, Yuan X, Feng R, Yang Z, Qi C (2016) *Int J Biol Macromol* 89:449
- Zhang Y, Shen Y, Chen Y, Yan Y, Pan J, Xiong Q, Shi W, Yu L (2016) *Chem Eng J* 294:222
- Huang K, Chai SH, Mayes RT, Tan S, Jones CW, Dai S (2016) *Microporous Mesoporous Mater* 230:100
- Brun N, Prabaharan SRS, Morcrette M, Sanchez C, Pécastaings G, Derré A, Soum A, Deleuze H, Birot M, Backov R (2009) *Adv Funct Mater* 19:3136
- Brun N, Prabaharan SRS, Morcrette M, Deleuze H, Birot M, Babot O, Achard MF, Surcin C, Backov R (2012) *J Phys Chem C* 116:1408
- Roberts AD, Li X, Zhang H (2014) *Chem Soc Rev* 43:4341
- Depardieu M, Janot R, Sanchez C, Bentaleb A, Demir-Cakan R, Gervais C, Birot M, Morcrette M, Backov R (2014) *J Mater Chem A* 2:18047
- Depardieu M, Demir-Cakan R, Sanchez C, Birot M, Deleuze H, Morcrette M, Backov R (2016) *Solid State Sci* 55:112
- Wang M, Yang H, Wang K, Chen S, Ci H, Shi L, Shan J, Xu S, Wu Q, Wang C, Tang M, Gao P, Liu Z, Peng H (2020) *Nano Lett* 20:2175
- Hwa Y, Kim HW, Shen H, Parkinson DY, McCloskey BD, Cairns EJ (2020) *Mater Horiz* 7:524
- Ma Y, Asfaw HD, Edström K (2015) *Chem Mater* 27:3957
- Jeonga H, Janga J, Jo C (2022) *Chem Eng J* 446:136860
- Boarettoa N, Garbayoa I, Valiyaveetil-SobhanRaj S, Quintela A, Li C, Casas-Cabanasa M, Aguesse F (2021) *J Power Sources* 502:229919
- Onsrud M, Tezel AO, Fotedar S, Svensson AM (2022) *SN Appl Sci* 4:225

44. Kovačič S, Jeřábek K, Krajnc P, Slugovc C (2012) *Polym Chem* 3:325
45. Kovačič S, Matsko NB, Jeřábek K, Krajnc P, Slugovc C (2013) *J Mater Chem A* 1:487
46. Kovačič S, Preishuber-Pflügl F, Slugovc C (2014) *Macromol Mater Eng* 299:843
47. Kovačič S, Schafzahl B, Matsko NB, Gruber K, Koller S, Schmuck M, Freunberger SA, Slugovc C (2022) *ACS Appl Energy Mater* 5:14381
48. Huang J, David A, Le Gac PY, Lorthioir C, Coelho C, Richaud E (2019) *Polym Degrad Stab* 166:258
49. Xiao W, Mi L, Cui S, Hou H, Chen W (2016) *New J Chem* 40:93
50. Tao X, Chen X, Xia Y, Huang H, Gan Y, Wu R, Chen F, Zhang W (2013) *J Mater Chem A* 1:3295
51. Oschatz M, Thieme S, Borchardt L, Lohe MR, Biemelt T, Bruckner J, Althues H, Kaskel S (2013) *Chem Commun* 49:5832
52. Patel MD, Cha E, Kang C, Gwalani B, Choi W (2017) *Carbon* 118:120
53. Oschatz M, Lee JT, Kim H, Nickel W, Borchardt L, Cho WI, Ziegler C, Kaskel S, Yushin G (2014) *J Mater Chem A* 2:17649
54. Wu C, Fu L, Maier J, Yu Y (2015) *J Mater Chem A* 3:9438
55. Shao Q, Zhu S, Chen J (2023). *Nano Res.* <https://doi.org/10.1007/s12274-022-5227-0>

**Publisher's Note** Springer Nature remains neutral with regard to jurisdictional claims in published maps and institutional affiliations.